8.4

COHERENT PROCESSING ACROSS MULTI-PRI WAVEFORMS

Mark E. Weber and Edward S. Chornoboy

MIT/Lincoln Lab
Lexington, Massachusetts

1. INTRODUCTION

Meteorological Doppler radars have typically utilized constant pulse-repetition intervals (PRI) to facilitate clutter filtering and estimation of weather echo spectral moments via pulse-pair or periodogram-based algorithms. Utilization of variable PRIs to support resolution of velocity ambiguities has been discussed, for example by Banjanin and Zrnic [1], but not implemented owing to difficulties associated with clutter filter design. Recent work by Chornoboy [2] presents design algorithms for time-varying finite impulse response (FIR) filters that achieve Chebyshev or mean-squared error (MSE) optimality when processing multi-PRI waveforms. This paper is a follow-on to that work, treating techniques for post-clutter filter processing (e.g. periodogram estimation) that are appropriate for such waveforms.

Our approach involves a least-squares fitting of the signal — sampled at a nonuniform rate — to a weighted sum of uniformly spaced sinusoids. The sinusoids or "basis functions" are chosen to span a Nyquist interval consistent with the longest PRI in the transmitted waveform, and need not be centered at zero Doppler. Determination of the sinusoid weightings — effectively a discrete Fourier transformation (DFT) — and the associated residual between the harmonic fit and the data are accomplished via multiplications of the signal vector with pre-computed matrices. The resulting spectrum estimate can be used directly for weather echo moment calculations, or can be inverse-Fourier transformed using conventional techniques to generate a time-domain signal representation.

This work has been motivated by a specific application — estimation of weather spectrum moments for a Wind Shear Processor (WSP) modification to the Federal Aviation Administration's Airport Surveillance Radar (ASR-9) [3]. Our approach supports candidate low-altitude radial wind estimation algorithms [3]–[6] that operate on frequency-domain signal representations and require that the radar's block-stagger PRI and the possibility of velocity ambiguities be accounted for in generating the spectrum estimates. In principle, however, these processing techniques are also applicable to weather radar systems such as WSR-88D and Terminal Doppler Weather Radar (TDWR) where range and Doppler ambiguities are an operational concern.

2. LEAST SQUARES HARMONIC FITTING

Data samples at arbitrary times t(n),

$$x_n = x[t(n)] \qquad n = 0,N-1 \qquad (1)$$

are modeled as the weighted sum of M harmonically related sinusoids:

$$\hat{x}_n = \sum_{m=0}^{m=M-1} y_m \exp\{i2\pi(f_o+m\Delta f)t(n)\} \quad . \quad (2)$$

Weights y_m are chosen so as to minimize the residual between the harmonic fit and the data samples:

$$\varepsilon^2 = \sum_{n=0}^{n=N-1} | x_n - \hat{x}_n |^2 \quad . \quad (3)$$

The solution and corresponding residual are:

$$\begin{aligned} \bar{y} &= \bar{A}\,\bar{x} \\ \varepsilon^2 &= \bar{x}^H \bar{B}\,\bar{x} \end{aligned} \qquad (4)$$

Here $\bar{y}$ is the M-length column vector of harmonic weights y_m and $\bar{x}$ is the N-length column vector of data samples. The MxN matrix $\bar{A}$ and the NxN matrix $\bar{B}$ are given by

$$\begin{aligned} \bar{A} &= (\bar{\Phi}^H\bar{\Phi})^{-1}\bar{\Phi}^H \\ \bar{B} &= \bar{I} - \bar{\Phi}\bar{A} \end{aligned} \qquad (5)$$

where basis function elements

$$\phi_{n,m} = \exp\{\, i2\pi(f_o+m\Delta f)t(n)\} \qquad (6)$$

define the NxM matrix Φ.

The following considerations establish the number, M, and spacing, Δf, of sinsuoids used to model the signal. First, the number of sinusoids must be less than or equal to the number of data samples so that the system of equations (2) is not underdetermined:

$$M \le N \quad . \quad (7)$$

Second, the transform of the frequency sampling "comb" (a comb in the time domain with spacing $1/\Delta f$) must not fold the signal over on itself:

$$\Delta f \le [t(N)-t(0)]^{-1} \quad . \quad (8)$$

Finally, the maximum signal bandwidth representable by the sinusoid set must be consistent with the longest PRI in the transmitted waveform:

$$M\Delta f \le [\max\{t(n)-t(n-1)\}]^{-1} \quad . \quad (9)$$

We choose Δf so as to satisfy the equality in equation (8), then

The work described has been sponsored by the Federal Aviation Administration. The U.S. Government assumes no liability for its contents or use thereof.

set M to be the largest integer that satisfies equation (9). This guarantees that condition (7) is satisfied.

3. APPLICATION TO ASR-9 WSP

The ASR-9 utilizes a variable PRI to mitigate "blind" speeds for aircraft targets. During the period in which the antenna scans one beamwidth in azimuth, a block of eight pulses is transmitted at a long PRI, followed by ten pulses at a short PRI. Because the antenna rotation rate of the ASR-9 varies under wind loading, "fill pulses" at the long PRI may be inserted following the two pulse blocks in to maintain scan-to-scan azimuth registration of the waveform. The ratio of the long and short PRIs is 9:7 with a typical value for the long PRI of 1 ms. The associated Nyquist interval for the S-band radar is 53 m/s.

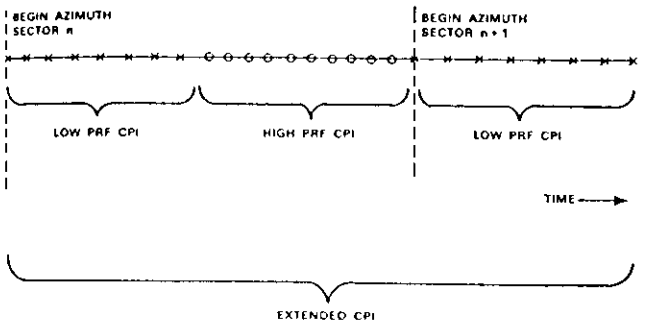

Figure 1. ASR-9 transmitted waveform.

In order to obtain a sufficient number of samples for clutter suppression and Doppler velocity estimation, the WSP operates coherently across three of the individual pulse blocks as shown. This "extended" coherent processing interval (CPI) spans 27 successive pulses and is the longest deterministic waveform available, owing to lack of *a priori* knowledge as to how many fill pulses will be inserted.

Figure 2 illustrates a candidate signal processing sequence used by the WSP to generate weather moment estimates. In-phase and quadrature signals are high-pass filtered using the shift-variant FIR designs described in [7]. Group delay is chosen so that the filter output sample spacing is equal to that of the input. Two samples at each end of the output data vector are discarded to minimize filter degradation at the beginning and end of the sequence. A first estimate of unambigous mean Doppler velocity is obtained through application of the "Chinese Remainder Theorem" to pulse-pair Doppler estimates obtained individually from the long- and short-PRI data blocks.

With a post-clutter filter data vector of length N=23, the conditions of equations (7) through (9) establish M=21 and $\Delta f = 48\ s^{-1}$ (2.5 m/s). Based on the Chinese Remainder Theorem estimate of unambiguous mean Doppler, one of two matrices $\bar{A}$, corresponding to basis functions with center frequency offsets f_o of respectively plus and minus 0.3 times the long-PRI Nyquist interval, is selected. Additional tests, described below, may be used to confirm that the selected basis function center frequency offset is appropriate. A "windowed" version (see below) of the matrix $\bar{A}$ is used to generate a spectrum estimate from the full 23-sample output of the clutter filter. Weather moment estimates, such as "low altitude" Doppler velocity [3]-[6], are generated from this full-resolution spectrum estimate.

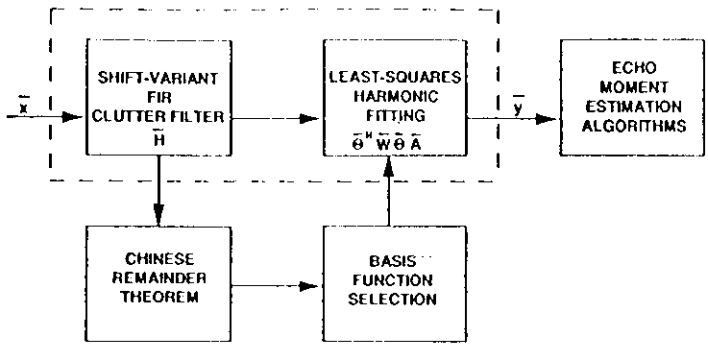

Figure 2. Block diagram of candidate signal processing sequence exploiting non-uniform PRI waveform for velocity ambiguity removal.

With this procedure, unaliased power spectrum estimates are obtained for weather signals between 0.8 and -0.8 times the long-PRI Nyquist interval. The resulting extended Nyquist interval (+/- 42 m/s) is sufficient for any weather conditions where aircraft landings or takeoffs would be attempted.

In the ASR-9 WSP application, resolution cells are revisited once every 5 seconds. Since weather parameters do not evolve this rapidly, the velocity ambiguity processing need not be repeated on every scan of the antenna (once per minute is sufficient). As shown by the dashed lines in Figure 2, on the remaining scans the matrix $\bar{A}$ can be preselected and cascaded with the matrix $\bar{H}$ that implements the shift-variant FIR filter.

Utilization of a matrix multiply to accomplish the signal processing leads to considerable flexibility. For example, clutter filtering, time-series data "windowing" and time-to-frequency transformation can be achieved through a single matrix multiply operation:

$$\bar{y} = \bar{\Theta}^{H} W \bar{\Theta} \bar{A} \bar{H} \bar{x} \qquad . \quad (10)$$

Here, the elements of $\bar{\Theta}$ are those of a conventional inverse DFT, and W is a square "windowing" matrix whose non-diagonal elements are zero, and whose diagonal elements are the desired window function. If zero-padding to obtain finer velocity spacing of spectrum estimates is desired, zeroes are appended to the columns of $\bar{\Theta}$ and the rows and columns of W, and $\bar{\Theta}^{H}$ is replaced by a square DFT matrix of appropriate order.

4. ILLUSTRATION OF MULTI-PRI PROCESSING

Figure 3 shows spectrum estimates for a sinsuoid of frequency 0.65 times the long-PRI Nyquist interval; the sinusoid has been sampled at 27 points corresponding to the ASR-9 waveform illustrated in Figure 1. The left and right panels are estimates generated using equation (10) with the above basis function offsets f_o of respectively minus and plus 0.3. The filter matrix $\bar{H}$ has been chosen to be all-pass in this example. The correct choice of basis function results in a spectrum with its peak correctly positioned and Doppler sidelobes that are consistent with theoretical performance of the Blackman taper used to construct the window matrix. Incorrect choice of f_o re-

sults in signficant whitening of the signal spectrum and an order of magnitude increase in the residual ε^2.

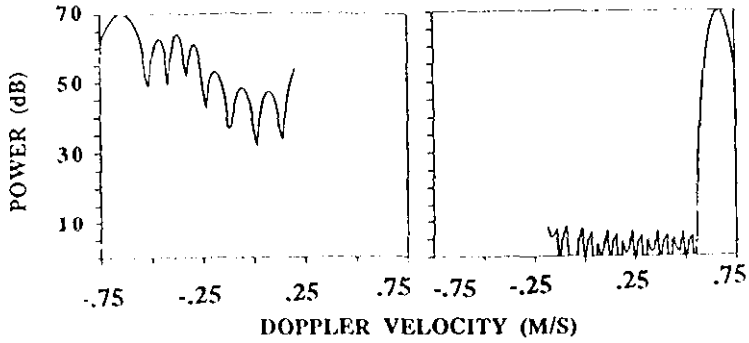

Figure 3. Spectrum estimates from equation (10) applied to simulated sinusoid sampled at non–equal intervals. Sinusoid normalized frequency is 0.65 and basis function offsets are –0.3 (left) and 0.3 (right).

Criteria testing the appropriateness of the choice of basis function frequency offset f_o can be used to reduce the likelihood of a gross unfolding error from the initial Chinese Remainder theorem Doppler estimate. As illustrated above, examples of such criteria are the magnitudes of the harmonic model residuals ε^2 and the "whiteness" (power ratio of minimum to maximum spectrum component) of the spectra estimated using different choices for f_o. Experiments using simulated weather signals with varying signal to noise, signal to clutter and spectrum widths have indicated that the "whiteness" test is generally more robuste.

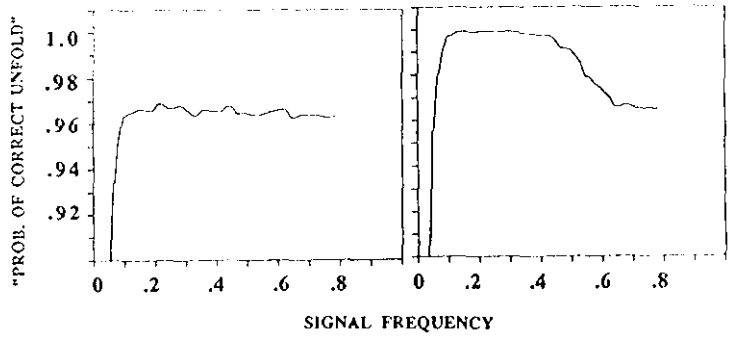

Figure 4. "Probability of correct unfold" as described in the text versus signal mean Doppler. The left panel treats the initial Chinese remainder theorem estimate. In the right panel, the "whiteness" test is used to affirm that this initial choice is appropriate

Figure 4 illustrates the concept. Monte Carlo simulations were run using a weather signal of moderate spectrum width (5 m/s) and low signal–to–noise ratio (5 dB) whose normalized mean Doppler frequency was varied from 0 to +0.8. The figure plots the probability that the positive basis function frequency offset is correctly selected. (Note that for signals with mean Doppler less than 0.2 minus the signal bandwidth, either choice for f_o is appropropriate). Our initial estimate (solid curve in the left panel) sets the sign of the selected basis function frequency offset equal to that of the Chinese Remainder theorem Doppler estimate and, in this example, is incorrect about 3.5% of the time. This estimate is checked against the choice for f_o that minimizes the "whiteness" of the resulting spectrum. The "whiteness" test complements the initial estimate by providing near perfect selection of basis function frequency offset as long as signal Doppler is not so high that significant power is outside the shifted Nyquist interval. When both tests are applied (right panel) the probability of selecting the appropriate sign of f_o, or flagging the data as suspect owing to disagreement, is near unity out to a normalized signal frequency of 0.5. At higher signal Doppler, the frequency offest selection accuracy degrades to the "baseline" value associated with the Chinese Remainder theorem. This degradation at high Doppler magnitude could be eliminated by testing of additional basis functions with larger frequency offsets (e.g. ± 0.9).

5. OTHER APPLICATIONS

Base data degradation produced by range and Doppler ambiguities remain a fundamental problem for weather radar, particularly with systems such as WSR–88D and TDWR where automated meteorological detection algorithms are used. The NEXRAD Technical Advisory committee recently identified range/Doppler ambiguities as the second highest priority unmet technical need (after data archiving). Initial Operational Test and Evaluation (OT&E) of the TDWR in Oklahoma City has likewise illustrated that second trip weather contamination and/or incorrectly dealiased radial velocity estimates may degrade the operational capabilities of the radar.

The work described here and in references [2] and [7] point the way to processing techniques that could ameliorate these problems when coupled with signal waveform changes. Reliable resolution of Doppler ambiguities would allow for operation at a lower average pulse repetition frequency, which in turn, would reduce the impact of range folding. While the signal processing requirements are considerable (approximately 200 MFLOPS in our ASR–9 application), rapid evolution in digital processing hardware capability makes such approaches feasible. We note, for example, that commercially available single–board array processing cards achieving this throughput are available for under $20,000.

REFERENCES

1. Z. Banjanin and D. Zrnic, Clutter rejection for Doppler weather radars which use staggered pulses. IEEE Transactions on Geoscience and Remote Sensing, 29, 610 620, 1991.

2. E. Chornoboy, Clutter filter design for multiple–PRT signals, Preprint Volume: 26th International Conference on Radar Meteorology, Norman, OK, May 24–28, 1993, AMS.

3. M. Weber, M. Stone, C. Primeggia, J. Anderson, Airport Surveillance Radar based wind shear detection, Preprint Volume: 4th International Conference on the Aviation Weather System, Paris, France, June 24 28, 1991, AMS.

4. D. Atlas, The detection of low level windshear with Airport Surveillance radar, 3rd International Conference on the Aviation Weather System, Anaheim, Ca., Jan 30 - Feb 3, 1989, AMS.

5. J. Anderson, Techniques for the detection of microburst outflows using Airport Surveillance Radars, 3rd International Conference on the Aviation Weather System, Anaheim, Ca., Jan 30 - Feb 3, 1989, AMS.

6. E. Chornoboy, Optimal mean velocity estimation for Doppler weather radars, IEEE Transactions on Geoscience and Remote Sensing, 32, 1993 (in press).

7. E Chornoboy, Addendum to "Ground Clutter Processing for Wind Measurements with Airport Surveillance Radars": Optimum Time–Varying Designs, Lincoln Laboratory Report ATC–191, 1993 (in press).